Missense suppressor mutations in 16S rRNA reveal the importance of helices h8 and h14 in aminoacyl-tRNA selection

SEAN P. MCCLORY,[1] JOSHUA M. LEISRING,[2] DAOMING QIN,[1] and KURT FREDRICK[1,2,3]

[1]Ohio State Biochemistry Program, The Ohio State University, Columbus, Ohio 43210, USA
[2]Department of Microbiology, The Ohio State University, Columbus, Ohio 43210, USA
[3]Center for RNA Biology, The Ohio State University, Columbus, Ohio 43210, USA

ABSTRACT

The molecular basis of the induced-fit mechanism that determines the fidelity of protein synthesis remains unclear. Here, we isolated mutations in 16S rRNA that increase the rate of miscoding and stop codon read-through. Many of the mutations clustered along interfaces between the 30S shoulder domain and other parts of the ribosome, strongly implicating shoulder movement in the induced-fit mechanism of decoding. The largest subset of mutations mapped to helices h8 and h14. These helices interact with each other and with the 50S subunit to form bridge B8. Previous cryo-EM studies revealed a contact between h14 and the switch 1 motif of EF-Tu, raising the possibility that h14 plays a direct role in GTPase activation. To investigate this possibility, we constructed both deletions and insertions in h14. While ribosomes harboring a 2-base-pair (bp) insertion in h14 were completely inactive in vivo, those containing a 2-bp deletion retained activity but were error prone. In vitro, the truncation of h14 accelerated GTP hydrolysis for EF-Tu bearing near-cognate aminoacyl-tRNA, an effect that can largely account for the observed miscoding in vivo. These data show that h14 does not help activate EF-Tu but instead negatively controls GTP hydrolysis by the factor. We propose that bridge B8 normally acts to counter inward rotation of the shoulder domain; hence, mutations in h8 and h14 that compromise this bridge decrease the stringency of aminoacyl-tRNA selection.

Keywords: ribosome; translation; EF-Tu; GTPase; decoding

INTRODUCTION

In order to faithfully translate the genetic code, the ribosome must select the correct (cognate) aminoacyl-tRNA (aa-tRNA) from the total cellular pool of aa-tRNAs in each round of elongation. This process, termed aa-tRNA selection or decoding, is facilitated by elongation factor Tu (EF-Tu), a three-domain GTPase that forms a ternary complex with GTP and aa-tRNA. Studies by Wintermeyer, Rodnina, and colleagues have led to the following model for decoding (for review, see Rodnina et al. 2005). The ternary complex initially interacts with the ribosome in a codon-independent manner, primarily through contacts to the 50S subunit. Then codon–anticodon pairing occurs in a 30S A site, which leads to activation of the GTPase domain of EF-Tu and GTP hydrolysis. Hydrolysis of GTP causes a large conformational change in the factor that leads to release of the aa-tRNA. The acceptor end of aa-tRNA then moves into the 50S subunit A site (a step termed accommodation), which is followed by a rapid peptide bond formation.

It has long been recognized that the thermodynamic stability of a cognate codon–anticodon interaction versus one with a single base-pair mismatch (near-cognate) cannot account for the accuracy of protein synthesis (for review, see Ogle and Ramakrishnan 2005; Rodnina et al. 2005). One way the translation machinery achieves high fidelity is by discriminating twice against near-cognate tRNA, once before and once after the functionally irreversible GTP hydrolysis step. This proofreading mechanism, though, is not maximally exploited to ensure high fidelity. Instead, the ribosome additionally employs an induced-fit mechanism in which cognate aa-tRNA accelerates two steps of the process—activation of EF-Tu for GTP hydrolysis and accommodation. Because this induced-fit mechanism increases rates for cognate aa-tRNA specifically, the ribosome can decode mRNA with both accuracy and speed.

Reprint requests to: Kurt Fredrick, Ohio State Biochemistry Program, The Ohio State University, 484 W. 12th Avenue, Columbus, OH 43210, USA; e-mail: fredrick.5@osu.edu; fax: (614) 292-8120.

Article published online ahead of print. Article and publication date are at http://www.rnajournal.org/cgi/doi/10.1261/rna.2228510.

The kinetic data imply that cognate codon–anticodon pairing induces a conformational change in the ribosomal complex that activates EF-Tu. Structural studies show that when cognate tRNA binds the ribosomal A site, three universally conserved 16S rRNA nucleotides (G530, A1492, and A1493) reorder to dock into the minor groove of the codon–anticodon helix (Ogle et al. 2001, 2002). This local rearrangement is accompanied by rotations of the 30S head and shoulder domains toward the subunit interface, conformational changes collectively described as "domain closure." Ramakrishnan and colleagues proposed that domain closure plays a central role in the induced-fit mechanism by promoting interactions between the ternary complex and ribosome that are critical for EF-Tu activation (Ogle and Ramakrishnan 2005). This domain closure model is supported by the observation that error-inducing antibiotics, such as paromomycin, stabilize the closed conformation of the ribosome and enhance forward rate constants for near-cognate tRNA (Pape et al. 2000; Ogle et al. 2002). Also, a number of ribosomal mutations that cause miscoding localize along the interface of S4 and S5 (Dahlgren and Ryden-Aulin 2000; Maisnier-Patin et al. 2002), ribosomal proteins that separate during domain closure (Ogle et al. 2001). These mutations are expected to destabilize the open state, decreasing the energy barrier for domain closure in the presence of near-cognate tRNA, consistent with their miscoding phenotypes.

While several lines of evidence support the domain closure model, some functional data are difficult to reconcile. In one study, certain mutations at the S4-S5 interface were found to make ribosomes hyperaccurate rather than error prone (Bjorkman et al. 1999). In a separate study, the effects of several S4 mutations on the level of S4-S5 binding were assessed using a yeast two-hybrid assay, and no correlation to translational accuracy was observed (Vallabhaneni and Farabaugh 2009). These unexpected data suggest that our understanding of aa-tRNA selection remains incomplete.

Genetic studies of ribosomal RNA have generally been hampered by the fact that most model organisms have multiple copies of the rRNA genes. In this work, using a specialized ribosome strain to bypass this issue, we have isolated and characterized a number of mutations in 16S rRNA that decrease the fidelity of translation elongation. Our findings strongly implicate shoulder movement in aa-tRNA selection and uncover the role of helices h8 and h14 in regulating GTP hydrolysis by EF-Tu.

RESULTS AND DISCUSSION

Isolation of missense and nonsense suppressor mutations in 16S rRNA

Using a specialized ribosome system described previously (Abdi and Fredrick 2005; Qin et al. 2007; Qin and Fredrick 2009), a classical genetic approach was taken to identify mutations in 16S rRNA that decrease the fidelity of translation elongation. Two screens were performed, one for missense suppressors and the other for nonsense (UGA) suppressors. To identify missense suppressors, we used indicator strain KLF4001, in which codon 461 of the reporter SD*(5′-AUCCC-3′)-*lacZ* gene was changed from GAA (Glu) to GAT (Asp). Glutamate 461 of β-galactosidase contributes to the active site, and an Asp substitution at this position abolishes enzymatic activity (Cupples and Miller 1988, 1989). Hence, the production of active β-galactosidase in the strain KLF4001 depends on misreading of the near-cognate GAU by Glu-tRNA. To identify nonsense suppressors, an indicator strain (KLF2723) containing TGA (stop) in place of TGG (Trp) at codon 585 of *lacZ* was used. In this strain, production of full-length LacZ requires the read-through of UGA. The two screens were done in an analogous way. Plasmid pKF207 encoding specialized 16S rRNA (ASD*: 5′-GGGGU-3′) was mutagenized by propagation in XL1-Red (Stratagene) and transformed into the appropriate indicator strain. Transformants were then screened on plates containing X-gal and arabinose for those expressing increased levels of β-galactosidase.

The results of these screens are shown in Table 1. A number of mutations were isolated in both screens, as was expected since ribosomes defective in aa-tRNA selection should increase misreading both GAU and UGA. With the exception of G886A, these mutations were distinct from those identified in an earlier screen for defects in initiation fidelity (Qin and Fredrick 2009). Nearly all of the mutations obtained were transitions. This bias seems to be due to the use of XL1-Red, because transversions engineered at several of these positions confer strong suppressor phenotypes that would have been easily detected in the screens (see below). Of the 34 mutations recovered, at least six (G886A, U911C, C1054U, C1200U, C1469U, and G1491A) were shown previously to influence the fidelity of elongation (Allen and Noller 1991; Gregory and Dahlberg 1995; Murgola et al. 1995; Lodmell and Dahlberg 1997; Pagel et al. 1997; Velichutina et al. 2000).

To verify that each mutation in Table 1 conferred a suppressor phenotype, site-directed mutagenesis was used to introduce each mutation into pKF207 de novo. The resulting plasmids were transformed into the appropriate indicator strain(s), and in each case, missense and/or nonsense suppression was confirmed. Then, the effects of these and a number of additional mutations on decoding fidelity in vivo were quantified (Fig. 1). To estimate the frequency of misreading (i.e., missense errors), the activity of β-galactosidase translated from *lacZ* (GAA 461 GAT) relative to that from *lacZ* (control) was determined for each of the mutant ribosomes. An analogous approach was taken to estimate the frequency of UGA read-through (i.e., nonsense errors) for a subset of the mutant ribosomes (Fig. 2). In general, the quantified error rate correlated with the number of times a given mutation was isolated in the corresponding screen (Table 1).

TABLE 1. Mutations in 16S rRNA that increase misreading of sense and stop codons

Mutation	Location	Number of independent isolates in each suppressor screen[a]	
		Missense[b]	Nonsense[c]
A7G	5′ end	2	0
A151G	h8	1	4
C153U	h8	1	0
G158A	h8	1	0
G159A	h8	6	0
A160G	h8	9	3
A161G	h8	8	3
A162G	h8	1	0
G168A	h8	2	0
U170A	h8	1	0
G299A	h12	15	5
A300G	h12	1	0
U343C	h14	1	0
ins345A[d]	h14	0	1
G346A	h14	3	0
G347A	h14	5	3
G347U	h14	1	0
ΔG348	h14	0	1
A349G	h14	1	0
ΔU420	h16	1	0
G423A	h16	0	1
G424A	h16	1	0
U598C	h21	1	0
G606A	h21	0	1
C634U	h21	4	6
G661A	h22	1	0
G886A	h27	1	0
U911C	h27	1	1
C1054U	h34	0	4
C1200U	h34	1	16
C1203U	h34	3	0
A1430G	h44	4	0
C1469U	h44	1	0
G1491A	h44	0	4

ins indicates insertion; Δ, deletion.
[a]Isolates were only considered independent if they originated from separate preparations of mutagenized pKF207.
[b]In this case, codon 461 of *lacZ* was changed from GAA to GAT. Production of active β-galactosidase requires misreading of GAU by Glu-tRNA.
[c]In this case, codon 585 of *lacZ* was changed from TGG to TGA. Production of active β-galactosidase requires read-through of UGA.
[d]Insertion of A after C345.

Elements of 16S rRNA involved in the fidelity of translation

The suppressor mutations clustered to distinct regions of 16S rRNA (Fig. 3). Three mutations (A7G, G299A, A300G) mapped to the solvent side of the subunit near the S4-S5 interface, where a number of protein mutations affecting fidelity have been previously localized (Fig. 3D; Bjorkman et al. 1999; Dahlgren and Ryden-Aulin 2000; Maisnier-Patin et al. 2002). Of these, G299A conferred the strongest phenotypes, increasing both missense and nonsense errors by approximately 10-fold (Figs. 1–2). Structural studies show that G299 normally pairs with the Hoogsteen face of G566, while the adjacent nucleotide A300 contacts U565 and C564 (Selmer et al. 2006). Nucleotides 564–566 are part of the 560 loop (nucleotides 557–566), which contains several sharp turns in its backbone and physically links the 5′ and central domains of 16S rRNA. O6 of G299 and O1P of G558 are involved in coordinating a magnesium ion that appears to stabilize the compressed fold of the 560 loop. Mutations A7G, G299A, and A300G are each predicted to destabilize these interactions between h12 and the 560 loop. Because these interactions lie where the shoulder domain interfaces with the remainder of the subunit, these mutations may increase miscoding by promoting domain closure, as has been proposed for S4/S5 mutations (Ogle and Ramakrishnan 2005). Pyrimidine substitutions were engineered at position 299, and these gave considerably weaker phenotypes than did G299A (Fig. 1). The fact that G299A confers the strongest phenotype might be explained by the electrostatic repulsion between N6 of the introduced A and the bound Mg^{2+}, which may destabilize the h12-560 loop interaction to the largest degree.

Three other mutations (U598C, G606A, and C634U) mapped nearby in h21 (Fig. 3D), and each of these caused a relatively modest (two- to fourfold) increase in miscoding (Fig. 1). From the platform domain, h21 spans across the backside of the subunit, and its terminal loop docks with elements of the shoulder domain (including h4, S4, and S16) (Selmer et al. 2006). Because h21 provides a structural support to the shoulder domain, it is plausible that these mutations in h21 affect shoulder rotation and it thereby confers their effects on decoding. Interestingly, U598 and C634 are located adjacent to His30 in S17, which is the location of a neamine resistance mutation that leads to a hyperaccurate phenotype (Bollen et al. 1975; Yaguchi et al. 1976).

Another group of mutations (ΔU420, G423A, and G424A) mapped in or adjacent to the UUCG tetraloop that caps h16 at the "top" of the shoulder domain (Fig. 3A–C), and these mutations increased miscoding by two- to threefold (Fig. 1). Deletions of 1 and 2 base pairs (bp) were engineered to shorten h16. Both of these truncations increased miscoding by about threefold, although the larger deletion was more deleterious to overall translation (Fig. 1). The tetraloop of h16 forms a contact with S3, a protein of the head domain. When the shoulder rotates during domain closure, this contact is partially disrupted as indicated by a 16% reduction of buried surface area (Ogle et al. 2001). Hence, these mutations are predicted to destabilize the open state of the 30S subunit, which may explain their miscoding phenotypes.

Two mutations mapped to h27 (G886A and U911C) (Fig. 3A), and each is predicted to change the G886-U911 wobble pair to a Watson–Crick pair. This region was previously implicated in translational fidelity (Lodmell and Dahlberg 1997), but the idea of a dynamic "switch" between two

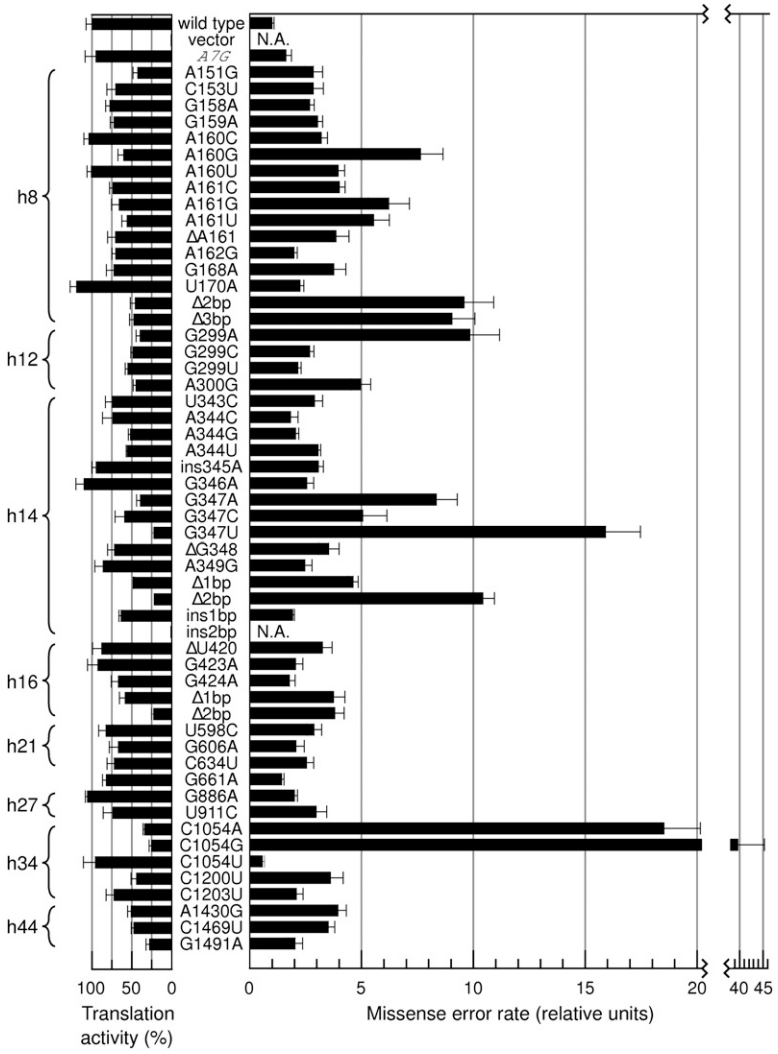

FIGURE 1. Effects of 16S rRNA mutations on missense suppression. Values on the leftward axis correspond to the relative levels of β-galactosidase translated from SD*-*lacZ* (control) mRNA by each of the mutant ribosomes (as indicated). Data represent the mean ± SEM from three or more independent experiments. Values on the rightward axis reflect the missense error rate, calculated as the level of active β-galactosidase produced from SD*-*lacZ* (GAA 461 GAT) divided by that from SD*-*lacZ* (control). For the wild-type specialized ribosomes, this quotient was 0.0013 ± 0.00008. The data shown correspond to the normalized quotient of two mean ± SE from three or more independent experiments. Mutations analyzed include those identified in the screens and those engineered. Prefixes "ins" and "Δ" denote insertion and deletion, respectively.

alternative base-pairing arrangements in this region has been ruled out (Rodriguez-Correa and Dahlberg 2004). These mutations lie at the junction of the major domains of the subunit, near the streptomycin-binding site.

Mutation C1054U was isolated four times in the nonsense suppressor screen (Table 1), consistent with a similar screen done in the past (Gregory and Dahlberg 1995). C1054U was not recovered as a missense suppressor, which was explained by the fact that the mutation decreased the misreading of GAU by twofold (Fig. 1). Mutations C1054A and C1054G, on the other hand, increased misreading by 20- and 40-fold, respectively. These purine substitutions also increased UGA read-through, although C1054A conferred the larger error rate in that case (Fig. 2). Structural studies have shown that C1054 contributes to the A site of the 30S subunit, contacting nucleotide 34 of tRNA and residues of release factors RF1 and RF2 (Ogle et al. 2001; Selmer et al. 2006; Korostelev et al. 2008; Laurberg et al. 2008; Weixlbaumer et al. 2008). The ability of mutations at position 1054 to increase read-through of stop codons is well established (Hanfler et al. 1990; Moine and Dahlberg 1994; Gregory and Dahlberg 1995; Murgola et al. 1995; Chernoff et al. 1996; Arkov et al. 1998), but whether these A-site mutations increase the frequency of the missense errors has been less clear. Murgola and colleagues failed to see effects of these mutations on misreading of several codons in *trpA* (Pagel et al. 1997). However, the relationship between the misreading error rate and the concentration of competing cognate aa-tRNA (Kramer and Farabaugh 2007) was unappreciated at that time, and the ability of ribosomal mutations to suppress those particular missense mutations was not demonstrated. Murgola and coworkers did see effects of 1054 mutations on the activities of several suppressor tRNAs that varied depending on the ribosomal mutation, suppressor tRNA, and/or *trpA* mutation (Pagel et al. 1997). Those experiments, involving missense suppression in the presence of a suppressor tRNA, essentially assess a competition between two cognate tRNAs and, hence, speak little to the question of decoding fidelity. Our data unambiguously show that C1054A and C1054G can decrease the fidelity of decoding in vivo (Fig. 1). The strong effects of C1054A and C1054G on both GUA misreading and UGA read-through suggest that these mutations may be generally detrimental to decoding fidelity. For example, a purine at 1054 may stabilize the near-cognate tRNA and/or reduce the energetic cost of domain closure in the presence of the near-cognate tRNA. Alternatively, C1054 may normally contribute to the uniformity of aa-tRNA selection (Ledoux and Uhlenbeck 2008; Ledoux et al. 2009), in which case mutations at this position would be expected to increase the rate of decoding for certain tRNAs and decrease the rate for others. This imbalance would lead to variable effects on missense suppression, which could explain the available data. Further experiments will be necessary to investigate these possibilities.

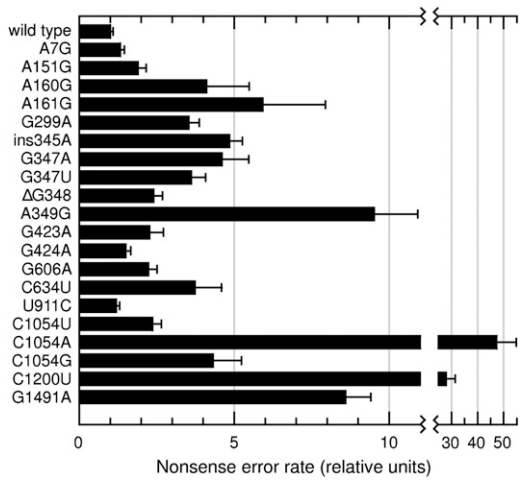

FIGURE 2. Effects of 16S rRNA mutations on nonsense suppression. Values reflect the rate of stop codon read-through, calculated as the level of active β-galactosidase produced from SD*-*lacZ* (TGG 586 TGA) divided by that from SD*-*lacZ* (control). For the wild-type specialized ribosomes, this quotient was 0.00096 ± 0.00007. The data shown correspond to the normalized quotient of two mean ± SE from three or more independent experiments.

Three other mutations (C1200U, C1203U, and G1491A) localized near the A site (Fig. 3E). Two of these (C1200U and G1491A) were isolated in previous screens for nonsense suppressors (Gregory and Dahlberg 1995; Murgola et al. 1995; Pagel et al. 1997) and conferred larger effects on UGA read-through than on GAU miscoding (Figs. 1, 2). The latter observation suggests that C1200U and G1491A inhibit RF2-dependent termination or enhance misreading by Trp-tRNA more than misreading by Glu-tRNA. All three mutations are predicted to perturb the A site in some way and thereby confer their phenotypes (Ogle et al. 2001; Selmer et al. 2006). N4 of C1200 donates a hydrogen bond to O1P of nucleotide 1055. The U substitution at 1200 precludes this interaction, potentially altering the conformation of the adjacent A-site nucleotide C1054. Nucleotide C1203 normally pairs with G1057, forming one of two Watson–Crick pairs that lie between loops (1054–1055 and 1200–1202) that bulge from opposite strands of h34. Mutation C1203U replaces this Watson–Crick pair with a wobble G–U pair, which may alter the position of nearby nucleotides such as C1200 and C1054. Nucleotide G1491 pairs with C1409 and lies adjacent to A-site nucleotides A1492 and A1493. These adenines rearrange when cognate tRNA binds the A site, moving out of h44 to dock into the minor groove of the codon–anticodon helix (Ogle et al. 2001). A1492 and A1493 also undergo substantial rearrangement upon release factor binding, although the resulting conformation is distinct from that induced by tRNA (Korostelev et al. 2008; Laurberg et al. 2008; Weixlbaumer et al. 2008). Mutation G1491A disrupts the 1409–1491 pair, which may affect these conformational changes of A1492 and A1493 important for decoding and/or termination.

Nearly half of the mutations mapped to either h8 or h14 (Table 1). These helices interact with each other near the EF-Tu binding site and contribute to intersubunit bridge B8 (Fig. 3F). Mutations with the strongest phenotypes were those of A160, A161, and G347 (Fig. 1). These residues are located at the interface between the two helices, suggesting that disruption or destabilization of this interface is responsible for the observed fidelity defects. Helix 14 contacts L19 and L14 of the 50S subunit to form bridge B8 (Yusupov et al. 2001; Selmer et al. 2006). Previous work identified two residues of L19 important for elongation fidelity (Maisnier-Patin et al. 2007). One of these residues, Q40, lies right next to the h14 contact site (Fig. 3F). The other residue, G104, also lies near the subunit interface, where L19 contacts h44 (Fig. 3F). Our missense suppressor screen identified two h44 mutations, A1430G and C1469U, which lie right in this vicinity (Table 1; Fig. 3F). The latter mutation was isolated previously as a suppressor of streptomycin dependence and was shown to increase misreading in vitro (Allen and Noller 1991).

Role of h8 and h14 in aa-tRNA selection

Recent cryo-EM studies provided evidence that EF-Tu interacts directly with h14 of 16S rRNA at the h8–h14 junction (Schuette et al. 2009; Villa et al. 2009). In those complexes, the antibiotic kirromycin was used to stabilize the ternary complex on the ribosome in a conformation believed to resemble the GTPase-activated state. On the ribosome, the switch 1 motif of the GTPase domain is repositioned away from the switch 2 and P-loop motifs in order to contact h14. This appears to open a hydrophobic "gate" that lies between the catalytic residue His84 and GTP in the ground (non-activated) state. These data raised the possibility that the interaction between h14 and switch 1 is important for activating GTP hydrolysis during decoding (Villa et al. 2009). To investigate this possibility, we constructed mutations that decrease or increase the helix length by 1 or 2 bp. The 2-bp deletion (h14Δ2), which should disrupt the putative switch 1 contact, decreased overall ribosome activity, but by only fivefold (Fig. 1). Furthermore, ribosomes carrying h14Δ2 were able to support growth of an *Escherichia coli* Δ7 prrn strain (see below). The fact that the h14Δ2 ribosomes retained substantial activity argues against an essential role for h14 in activating EF-Tu. In contrast, lengthening h14 by 2 bp completely abolishes translation activity in vivo (Fig. 1). Normally, the end of h14 butts up against L19 and L14 to form bridge B8 (Fig. 3F). A 2-bp extension of h14 is predicted to push the subunits apart in this region, a condition that appears to be intolerable for translation.

Although active, h14Δ2 ribosomes were found to be error prone, misreading GAU at a rate 10-fold higher than that of control ribosomes (Fig. 1). We also constructed 2- and 3-bp deletions in h8 (h8Δ2 and h8Δ3), each of which should disrupt its contact to h14 but still allow potential interactions

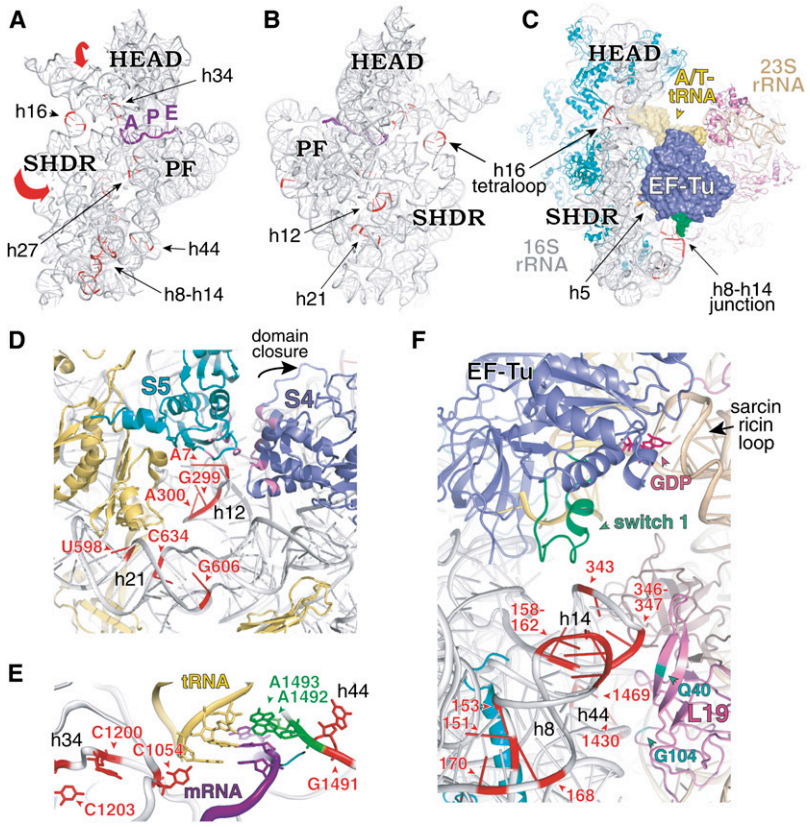

FIGURE 3. Where the mutations map. An overview of the locations of the mutations (depicted in red throughout) on the tertiary structure of 16S rRNA (PDB 2WRN) viewed from the interface (*A*) and solvent (*B*) perspective. Large red arrows in panel *A* indicate movements of 30S head and shoulder (SHDR) domains with respect to the platform (PF) during domain closure. (*C*) Cryo-EM reconstruction of the ternary complex bound to the 70S ribosome in the presence of kirromycin (Protein Data Bank [PDB] 3FIH and 3FIK). The modeled switch 1 motif of EF-Tu is shown in green near the h8-h14 junction. (*D*) Solvent view of the 30S subunit (PDB 2AVY) showing mutations found in h12 and h21. Mutations isolated previously in proteins S4 and S5 (Maisnier-Patin et al. 2002) are indicated in pink. (*E*) View of the 30S A site (PDB 2WRN) showing locations of mutations in the vicinity. (*F*) Closer view of the complex shown in panel *C*, showing locations of mutations found in h8, h14, and h44 (PDB 3FIH and 3FIK). Mutations in protein L19 that decrease fidelity (Maisnier-Patin et al. 2007) are indicated in turquoise.

between h14 and EF-Tu to form. These mutant ribosomes exhibited phenotypes very similar to the h14Δ2 mutant (Fig. 1), suggesting that disruption of the h8–h14 interface is sufficient for loss of fidelity.

How does disruption of the h8–h14 interface affect aa-tRNA selection? To address this question, we introduced mutations h14Δ2, h8Δ3, and G347U into an *E. coli* Δ7 prrn strain, purified the corresponding mutant 70S ribosomes, and analyzed their activities in the initial selection phase of decoding (i.e., EF-Tu-dependent GTP hydrolysis) (Fig. 4). Mutation G347U was included because it had the largest decoding defect among the collection of h8/h14 mutations (Fig. 1). Previous work by Rodnina and colleagues indicates that initial selection can be represented by a three-step kinetic model, in which initial binding of the ternary complex (step 1) is followed by codon recognition (step 2), which is followed by GTPase activation/GTP hydrolysis (step 3) (Pape et al. 1998, 1999; Gromadski and Rodnina 2004; Gromadski et al. 2006). The hydrolysis event itself is very rapid and so can be grouped with the GTPase activation in the scheme. In the near-cognate case, step 3 is much slower than step 2 and hence is rate limiting for the overall reaction. In the cognate case, steps 2 and 3 occur at comparable rates; hence, each is partially rate limiting for the overall reaction. Ribosome complexes programmed with either UUU (cognate) or CUU (near-cognate) in the A site (at various concentrations ≥0.5 μM) were rapidly mixed with EF-Tu•[γ-^{32}P]GTP•Phe-tRNA^{Phe} (<0.3 μM), and the rate of single-turnover GTP hydrolysis was determined. Apparent rates were plotted versus ribosome concentration, and the data were fit to obtain parameters k_{GTPmax}, the maximal rate of GTP hydrolysis, and $K_{1/2}$, the concentration of ribosomes at which half-maximal rate was observed. We found that each mutation stimulated GTP hydrolysis, increasing k_{GTPmax} by five- to eightfold in the near-cognate case and by two- to threefold in the cognate case (Fig. 4; Table 2). In the framework of the Rodnina model, these data suggest that the mutations increase k_3 (GTPase activation). The large effects on k_{GTPmax} seen in the near-cognate case can only be explained with an increase in k_3. In the cognate case, a similar increase in k_3 would be expected to increase k_{GTPmax} more modestly and increase $K_{1/2}$, and both of these effects are observed. Effects on step 2 (e.g., an increase in k_2 and/or decrease in k_{-2}) could also contribute to the observed increases in k_{GTPmax}, so additional experiments will be necessary to elucidate more precisely how initial selection is perturbed by these mutations. Nonetheless, these data are clearly inconsistent with the idea that h14 helps activate the GTPase domain of EF-Tu. Instead, these data suggest that h14 acts with h8 to negatively regulate GTP hydrolysis and thereby increase the stringency of decoding.

We propose that intersubunit bridge B8 normally acts to counter inward rotation of the 30S shoulder domain, a conformational change critical for GTPase activation. Any mutations in h8, h14, and L19 that compromise the bridge would reduce the energetic cost of inward shoulder rotation, allowing higher rates of GTP hydrolysis in the

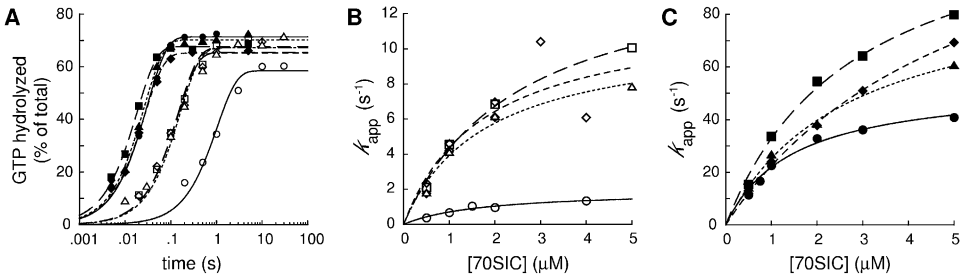

FIGURE 4. Effects of mutations in helices h8 and h14 on initial selection. 70S initiation complexes (70SIC) programmed with either cognate UUU (closed symbols) or near-cognate CUU (open symbols) in the A site were rapidly mixed with EF-Tu•[γ-^{32}P]GTP•Phe-tRNA^{Phe}, and rates of GTP hydrolysis were determined. Wild type indicated by ●/○ and solid lines; G347U, ■/□ and long dashed lines;h14Δ2, ◆/◇ and medium dashed lines; and h8Δ3, ▲/△ and short dashed lines. (*A*) Examples of time courses at 2 μM 70SIC. Data were fit to a single exponential function to obtain the apparent rates of GTP hydrolysis (k_{app}). Apparent rates for near-cognate tRNA (*B*) and cognate tRNA (*C*) plotted versus [70SIC]. Data were fit to the equation $k_{app} = k_{GTPmax}•[70SIC]/(K_{1/2} + [70SIC])$, yielding the parameters shown in Table 2.

absence of a cognate codon–anticodon interaction and hence higher error rates. The idea that small changes in intersubunit distance in this region play a key role in decoding is supported by structural studies (Ogle and Ramakrishnan 2005) and our observation that a 2-bp extension of h14 results in complete loss of translation activity (Fig. 1). Mutations in h44 and L19, which lie at the section of bridge B6 closest to B8 (Fig. 3F), are also likely to reduce constraints on shoulder rotation, and hence their effects on fidelity can also be rationalized with this simple model.

The ratio of cognate $k_{GTPmax}/K_{1/2}$ to near-cognate $k_{GTPmax}/K_{1/2}$ was calculated to estimate the effects of mutations h14Δ2, h8Δ3, and G347U on the fidelity of initial selection (Table 2). For control ribosomes, this ratio was 34, in line with previous studies (Gromadski and Rodnina 2004; Ledoux and Uhlenbeck 2008). The mutations reduced this ratio by four- to ninefold, generally consistent with their fidelity defects in vivo. These estimated effects on the initial selectivity, though, cannot completely account for the decoding defects observed in vivo, and the trend h14Δ2 > h8Δ3 > G347U seen in vitro differs from that (G347U > h14Δ2 ≈ h8Δ3) seen in vivo (Table 2). These differences may stem from the different tRNA species involved in the assays and/or additional effects on the proofreading stage of decoding.

The ability of these ribosomal mutations to stimulate EF-Tu raises the question of whether translation elongation is increased as a consequence. Our data do not address this question. The steady-state rate of product yield (e.g., translation activity in Fig. 1) is normally limited by initiation rather than elongation. An increase in the elongation rate would be predicted to decrease the density of ribosomes on the *lacZ* mRNA with little or no effect on the overall rate of product yield (Arava et al. 2003, 2005). Experiments that directly measure the elongation rate will be necessary to determine which mutations affect the speed of translation (Sorensen and Pedersen 1991; Mitarai et al. 2008).

Ribosomes harboring G347U, h14Δ2, or h8Δ3 were able to support growth in the Δ7 prrn strain, although the rate of growth in these strains was reduced by 15%, 33%, and 14%, respectively (data not shown). These data show that *E. coli* can tolerate quite low translational fidelity, at least when grown on rich media in the laboratory. Interestingly, we have constructed Δ7 prrn strains with mutations C1054A (18% reduced growth rate) and C1054U (6% reduced growth rate) but were unsuccessful in our attempts to make Δ7 prrn (C1054G) (Shoji et al. 2009). It is tempting to speculate that C1054G, which causes a 40-fold increase in misreading by Glu-tRNA (Fig. 1), decreases the accuracy of decoding below the minimal threshold required for viability.

Importance of h5 in translation

The data described above provide functional evidence that movement of the shoulder domain plays a critical role in the accuracy of decoding. Clues to how shoulder rotation may activate the GTPase domain of EF-Tu come from a recent 3.6 Å resolution crystal structure of the ternary complex bound to the ribosome (Schmeing et al. 2009). This complex was stabilized by kirromycin and hence is quite analogous to

TABLE 2. Kinetic parameters for EF-Tu–dependent GTP hydrolysis on control and mutant ribosomes

	Cognate		Near-cognate		
Ribosomes	k_{GTPmax} (sec^{-1})	$K_{1/2}$ (μM)	k_{GTPmax} (sec^{-1})	$K_{1/2}$ (μM)	Initial selectivity[a]
Control	54 ± 3	1.5 ± 0.2	1.9 ± 0.3	1.8 ± 0.6	34
G347U	130 ± 10	2.8 ± 0.5	15 ± 1	2.5 ± 0.4	7.7
h14Δ2	140 ± 10	5.4 ± 0.6	12 ± 4	1.8 ± 1	3.9
h8Δ3	93 ± 6	2.7 ± 0.3	11 ± 1	1.8 ± 0.5	5.6

Values and their standard errors were calculated from the curve fits shown in Figure 4.
[a](Cognate $k_{GTPmax}/K_{1/2}$)/(Near-cognate $k_{GTPmax}/K_{1/2}$).

those solved by cryo-EM; however, in the crystals, the switch 1 region of EF-Tu was completely disordered. A number of specific conformational changes in tRNA and EF-Tu could be inferred by the high-resolution co-crystal structure. When the cognate ternary complex binds the ribosome, the tRNA adopts a distorted conformation—its anticodon stem bends and exhibits less helical twist, while its 3′ end rearranges to make specific contacts with h5 of the shoulder domain of the 30S subunit. Two regions of domain 2 of EF-Tu (residues 256–273 and 219–226) also change position in order to interact with h5 of the shoulder. It was proposed that these conformational changes, stabilized by the shoulder in the closed state, disrupt an interaction between switch 1 and the 3′ end of tRNA to open the hydrophobic gate and activate the GTPase domain of EF-Tu (Schmeing et al. 2009). The effects of the mutation G222D of EF-Tu lend support to this model (Vorstenbosch et al. 1996). This mutation, which is predicted to disrupt the contacts between domain 2 of EF-Tu and h5 of 16S rRNA, specifically blocks the GTPase activation step of decoding (Vorstenbosch et al. 1996).

To investigate the potential importance of h5 in decoding, we targeted several nucleotides that contact the residues of EF-Tu and/or tRNA. Base substitutions were generated at positions 55, 357, and 367, and their effects on translation activity were quantified using our specialized ribosome system (Fig. 5). Most of these mutations reduced ribosome activity to background levels. Some residual activity (2%–6% of the control) was seen for certain substitutions at positions 357 and 367, but in no case was ribosome activity high enough to assess the fidelity of elongation. These data show that these h5 nucleotides, particularly A55, are critical for translation, in line with the model proposed by Ramakrishnan and coworkers (Schmeing et al. 2009). It is important to point out, though, that these data reflect the overall translation activity as opposed to the decoding step in isolation. Further experiments will be necessary to determine the degree to which these h5 mutations influence decoding and other steps in protein synthesis.

Conclusions

Here, we report the first screen for missense suppressor mutations in 16S rRNA. Most of the mutations mapped near interfaces between the 30S shoulder domain and other parts of the ribosome, strongly implicating shoulder movement in the molecular mechanism of decoding. The largest cluster of mutations localized to helices h8 and h14, which contact each other to form the 30S portion of bridge B8. While ribosomes carrying a 2-bp extension of h14 were completely inactive, those with a truncation of either h14 or h8 were error prone and exhibited elevated rates of GTP hydrolysis by EF-Tu. These data argue against a critical role for h14 in activating EF-Tu and suggest instead that h14 acts with h8 to negatively regulate GTP hydrolysis and thereby increase the stringency of aa-tRNA selection.

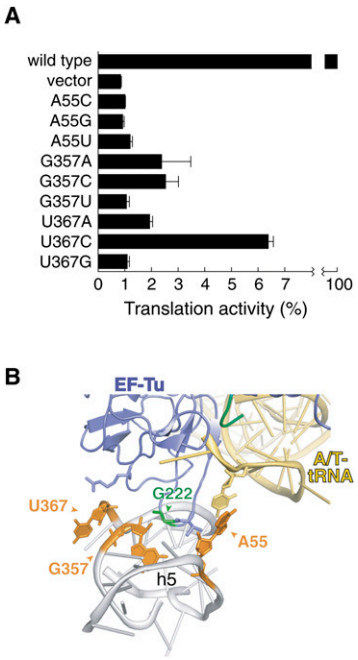

FIGURE 5. Effects of mutations in helix 5 on translation activity in vivo. (*A*) Values correspond to the relative levels of β-galactosidase translated from SD*-*lacZ* (control) mRNA by each of the mutant ribosomes (as indicated). The background level of β-galactosidase, determined from cells lacking specialized ribosomes (vector), is approximately 1%. Data represent the mean ± SEM from three or more independent experiments. (*B*) Interaction of h5 with domain 2 of EF-Tu and the 3′-CCA end of the A/T-tRNA (PDB ZWRN). The location of a G222D mutation, which impairs GTPase activation (Vorstenbosch et al. 1996), is indicated in green.

MATERIALS AND METHODS

Bacterial strains

Indicator strains KLF4001, KLF2723, and KLF2674 carry the *lacZ* reporter in single copy on the chromosome and were constructed from parental strain CSH142 [F- *ara Δ(gpt-lac)5*] as described previously (Abdi and Fredrick 2005; Qin et al. 2007). In these strains, *lacZ* is preceded by the alternative Shine–Dalgarno (SD) sequence 5′-ATCCC-3′ (SD*) and is under transcriptional control of a consensus P_{ant} promoter. In KLF4001, *lacZ* carries a missense mutation at codon 461 (GAA to GAT). In KLF2723, *lacZ* contains a UGA stop at codon 585. In KLF2674, *lacZ* contains no mutations (control strain). These indicator strains were made *recA*$^-$ by P1 transduction using donor strain JC14604 [*Δ(recA-srl)306*, *srlR301::Tn10*] obtained from the E. coli Genetic Stock Center (Yale University). *E. coli* Δ7 prrn strains were made using SQZ10 as described previously (Qin et al. 2007).

Engineered mutations

The precise nature of the deletion mutations constructed in 16S rRNA are as follows: h8Δ2bp, Δ(154,155,166,167); h8Δ3bp, Δ(154,155,157,164,166,167); h14Δ1bp, Δ(340,349); h14Δ2bp, Δ(340,341,348,349); h16Δ1bp, Δ(418,425); and h16Δ2bp, Δ(417,418,425,426). For the insertion mutations in h14, either

one (h14ins1bp) or two (h14ins2bp) additional C–G pairs were added in the middle of the helix.

Genetic screens

The genetic screens were performed as described previously (Qin and Fredrick 2009), except that indicator strains KLF4001 and KLF2723 were used. Mutator strain XL1-Red (Stratagene) was employed for the mutagenesis. Although the results of the screens suggested a bias for transitions in the mutagenesis, we did not perform a thorough analysis of the method with regard to mutation frequency or positional distribution.

β-Galactosidase assays

β-Galactosidase activity was measured as described previously (Abdi and Fredrick 2005; Qin et al. 2007), using the substrate *o*-nitrophenyl-β-D-galactopyranoside (ONPG; Sigma) for experiments involving missense suppression and chlorophenol red-β-D-galactopyranoside (CPRG; Sigma) for those involving nonsense suppression. ONPG was chosen in the former case because the E461D mutant of LacZ cannot hydrolyze ONPG (Cupples et al. 1990) but has residual activity on other substrates (Cupples and Miller 1988) that could potentially mask miscoding events in our experimental system (Cupples and Miller 1988; Cupples et al. 1990). This was not an issue for nonsense suppression (because the truncated LacZ is inactive on all substrates), so CRPG was used for increased sensitivity.

Kinetic assays

GTP hydrolysis measurements were performed as described (Ledoux and Uhlenbeck 2008), except that reactions were carried out in polymix buffer (Ehrenberg et al. 1990). The mRNAs were the same as those used in a previous study (Ling et al. 2007).

ACKNOWLEDGMENTS

We thank C. Squires and S. Quan for *E. coli* strain SQZ10 and J. Ling for providing purified mRNA. This work was supported by National Institutes of Health grant no. GM072528.

Received April 19, 2010; accepted June 27, 2010.

REFERENCES

Abdi NM, Fredrick K. 2005. Contribution of 16S rRNA nucleotides forming the 30S subunit A and P sites to translation in *Escherichia coli*. *RNA* **11:** 1624–1632.

Allen PN, Noller HF. 1991. A single base substitution in 16S ribosomal RNA suppresses streptomycin dependence and increases the frequency of translational errors. *Cell* **66:** 141–148.

Arava Y, Wang Y, Storey JD, Liu CL, Brown PO, Herschlag D. 2003. Genome-wide analysis of mRNA translation profiles in *Saccharomyces cerevisiae*. *Proc Natl Acad Sci* **100:** 3889–3894.

Arava Y, Boas FE, Brown PO, Herschlag D. 2005. Dissecting eukaryotic translation and its control by ribosome density mapping. *Nucleic Acids Res* **33:** 2421–2432.

Arkov AL, Freistroffer DV, Ehrenberg M, Murgola EJ. 1998. Mutations in RNAs of both ribosomal subunits cause defects in translation termination. *EMBO J* **17:** 1507–1514.

Bjorkman J, Samuelsson P, Andersson DI, Hughes D. 1999. Novel ribosomal mutations affecting translational accuracy, antibiotic resistance, and virulence of *Salmonella typhimurium*. *Mol Microbiol* **31:** 53–58.

Bollen A, Cabezon T, de Wilde M, Villarroel R, Herzog A. 1975. Alteration of ribosomal protein S17 by mutation linked to neamine resistance in *Escherichia coli*. I. General properties of neaA mutants. *J Mol Biol* **99:** 795–806.

Chernoff YO, Newnam GP, Liebman SW. 1996. The translational function of nucleotide C1054 in the small subunit rRNA is conserved throughout evolution: Genetic evidence in yeast. *Proc Natl Acad Sci* **93:** 2517–2522.

Cupples CG, Miller JH. 1988. Effects of amino acid substitutions at the active site in *Escherichia coli* β-galactosidase. *Genetics* **120:** 637–644.

Cupples CG, Miller JH. 1989. A set of *lacZ* mutations in *Escherichia coli* that allow rapid detection of each of the six base substitutions. *Proc Natl Acad Sci* **86:** 5345–5349.

Cupples CG, Miller JH, Huber RE. 1990. Determination of the roles of Glu-461 in β-galactosidase (*Escherichia coli*) using site-specific mutagenesis. *J Biol Chem* **265:** 5512–5518.

Dahlgren A, Ryden-Aulin M. 2000. A novel mutation in ribosomal protein S4 that affects the function of a mutated RF1. *Biochimie* **82:** 683–691.

Ehrenberg M, Bilgin N, Kurland CG. 1990. Design and use of a fast and accurate in vitro translation system. In *Ribosomes and protein synthesis*, (ed. G Spedding), pp. 101–129. IRL Press, Oxford, UK.

Gregory ST, Dahlberg AE. 1995. Nonsense suppressor and antisuppressor mutations at the 1409–1491 base pair in the decoding region of *Escherichia coli* 16S rRNA. *Nucleic Acids Res* **23:** 4234–4238.

Gromadski KB, Rodnina MV. 2004. Kinetic determinants of high-fidelity tRNA discrimination on the ribosome. *Mol Cell* **13:** 191–200.

Gromadski KB, Daviter T, Rodnina MV. 2006. A uniform response to mismatches in codon–anticodon complexes ensures ribosomal fidelity. *Mol Cell* **21:** 369–377.

Hanfler A, Kleuvers B, Goringer HU. 1990. The involvement of base 1054 in 16S rRNA for UGA stop codon dependent translational termination. *Nucleic Acids Res* **18:** 5625–5632.

Korostelev A, Asahara H, Lancaster L, Laurberg M, Hirschi A, Zhu J, Trakhanov S, Scott WG, Noller HF. 2008. Crystal structure of a translation termination complex formed with release factor RF2. *Proc Natl Acad Sci* **105:** 19684–19689.

Kramer EB, Farabaugh PJ. 2007. The frequency of translational misreading errors in *E. coli* is largely determined by tRNA competition. *RNA* **13:** 87–96.

Laurberg M, Asahara H, Korostelev A, Zhu J, Trakhanov S, Noller HF. 2008. Structural basis for translation termination on the 70S ribosome. *Nature* **454:** 852–857.

Ledoux S, Uhlenbeck OC. 2008. Different aa-tRNAs are selected uniformly on the ribosome. *Mol Cell* **31:** 114–123.

Ledoux S, Olejniczak M, Uhlenbeck OC. 2009. A sequence element that tunes *Escherichia coli* $tRNA_{GGC}^{Ala}$ to ensure accurate decoding. *Nat Struct Mol Biol* **16:** 359–364.

Ling J, Yadavalli SS, Ibba M. 2007. Phenylalanyl-tRNA synthetase editing defects result in efficient mistranslation of phenylalanine codons as tyrosine. *RNA* **13:** 1881–1886.

Lodmell JS, Dahlberg AE. 1997. A conformational switch in *Escherichia coli* 16S ribosomal RNA during decoding of messenger RNA. *Science* **277:** 1262–1267.

Maisnier-Patin S, Berg OG, Liljas L, Andersson DI. 2002. Compensatory adaptation to the deleterious effect of antibiotic resistance in *Salmonella typhimurium*. *Mol Microbiol* **46:** 355–366.

Maisnier-Patin S, Paulander W, Pennhag A, Andersson DI. 2007. Compensatory evolution reveals functional interactions between ribosomal proteins S12, L14, and L19. *J Mol Biol* **366:** 207–215.

Mitarai N, Sneppen K, Pedersen S. 2008. Ribosome collisions and translation efficiency: Optimization by codon usage and mRNA destabilization. *J Mol Biol* **382:** 236–245.

Moine H, Dahlberg AE. 1994. Mutations in helix 34 of *Escherichia coli* 16 S ribosomal RNA have multiple effects on ribosome function and synthesis. *J Mol Biol* **243:** 402–412.

Murgola EJ, Pagel FT, Hijazi KA, Arkov AL, Xu W, Zhao SQ. 1995. Variety of nonsense suppressor phenotypes associated with mutational changes at conserved sites in *Escherichia coli* ribosomal RNA. *Biochem Cell Biol* **73:** 925–931.

Ogle JM, Ramakrishnan V. 2005. Structural insights into translational fidelity. *Annu Rev Biochem* **74:** 129–177.

Ogle JM, Brodersen DE, Clemons WM Jr, Tarry MJ, Carter AP, Ramakrishnan V. 2001. Recognition of cognate transfer RNA by the 30S ribosomal subunit. *Science* **292:** 897–902.

Ogle JM, Murphy FV, Tarry MJ, Ramakrishnan V. 2002. Selection of tRNA by the ribosome requires a transition from an open to a closed form. *Cell* **111:** 721–732.

Pagel FT, Zhao SQ, Hijazi KA, Murgola EJ. 1997. Phenotypic heterogeneity of mutational changes at a conserved nucleotide in 16 S ribosomal RNA. *J Mol Biol* **267:** 1113–1123.

Pape T, Wintermeyer W, Rodnina MV. 1998. Complete kinetic mechanism of elongation factor Tu-dependent binding of aminoacyl-tRNA to the A site of the *E. coli* ribosome. *EMBO J* **17:** 7490–7497.

Pape T, Wintermeyer W, Rodnina M. 1999. Induced fit in initial selection and proofreading of aminoacyl-tRNA on the ribosome. *EMBO J* **18:** 3800–3807.

Pape T, Wintermeyer W, Rodnina MV. 2000. Conformational switch in the decoding region of 16S rRNA during aminoacyl-tRNA selection on the ribosome. *Nat Struct Biol* **7:** 104–107.

Qin D, Fredrick K. 2009. Control of translation initiation involves a factor-induced rearrangement of helix 44 of 16S ribosomal RNA. *Mol Microbiol* **71:** 1239–1249.

Qin D, Abdi NM, Fredrick K. 2007. Characterization of 16S rRNA mutations that decrease the fidelity of translation initiation. *RNA* **13:** 2348–2355.

Rodnina MV, Gromadski KB, Kothe U, Wieden HJ. 2005. Recognition and selection of tRNA in translation. *FEBS Lett* **579:** 938–942.

Rodriguez-Correa D, Dahlberg AE. 2004. Genetic evidence against the 16S ribosomal RNA helix 27 conformational switch model. *RNA* **10:** 28–33.

Schmeing TM, Voorhees RM, Kelley AC, Gao YG, Murphy FVt, Weir JR, Ramakrishnan V. 2009. The crystal structure of the ribosome bound to EF-Tu and aminoacyl-tRNA. *Science* **326:** 688–694.

Schuette JC, Murphy FVt, Kelley AC, Weir JR, Giesebrecht J, Connell SR, Loerke J, Mielke T, Zhang W, Penczek PA, et al. 2009. GTPase activation of elongation factor EF-Tu by the ribosome during decoding. *EMBO J* **28:** 755–765.

Selmer M, Dunham CM, Murphy FVt, Weixlbaumer A, Petry S, Kelley AC, Weir JR, Ramakrishnan V. 2006. Structure of the 70S ribosome complexed with mRNA and tRNA. *Science* **313:** 1935–1942.

Shoji S, Abdi NM, Bundschuh R, Fredrick K. 2009. Contribution of ribosomal residues to P-site tRNA binding. *Nucleic Acids Res* **37:** 4033–4042.

Sorensen MA, Pedersen S. 1991. Absolute in vivo translation rates of individual codons in *Escherichia coli*. The two glutamic acid codons GAA and GAG are translated with a threefold difference in rate. *J Mol Biol* **222:** 265–280.

Vallabhaneni H, Farabaugh PJ. 2009. Accuracy modulating mutations of the ribosomal protein S4-S5 interface do not necessarily destabilize the rps4-rps5 protein-protein interaction. *RNA* **15:** 1100–1109.

Velichutina IV, Dresios J, Hong JY, Li C, Mankin A, Synetos D, Liebman SW. 2000. Mutations in helix 27 of the yeast *Saccharomyces cerevisiae* 18S rRNA affect the function of the decoding center of the ribosome. *RNA* **6:** 1174–1184.

Villa E, Sengupta J, Trabuco LG, LeBarron J, Baxter WT, Shaikh TR, Grassucci RA, Nissen P, Ehrenberg M, Schulten K, et al. 2009. Ribosome-induced changes in elongation factor Tu conformation control GTP hydrolysis. *Proc Natl Acad Sci* **106:** 1063–1068.

Vorstenbosch E, Pape T, Rodnina MV, Kraal B, Wintermeyer W. 1996. The G222D mutation in elongation factor Tu inhibits the codon-induced conformational changes leading to GTPase activation on the ribosome. *EMBO J* **15:** 6766–6774.

Weixlbaumer A, Jin H, Neubauer C, Voorhees RM, Petry S, Kelley AC, Ramakrishnan V. 2008. Insights into translational termination from the structure of RF2 bound to the ribosome. *Science* **322:** 953–956.

Yaguchi M, Wittmann HG, Cabezon T, DeWilde M, Villarroel R, Herzog A, Bollen A. 1976. Alteration of ribosomal protein S17 by mutation linked to neamine resistance in *Escherichia coli*. II. Localization of the amino acid replacement in protein S17 from a meaA mutant. *J Mol Biol* **104:** 617–620.

Yusupov MM, Yusupova GZ, Baucom A, Lieberman K, Earnest TN, Cate JH, Noller HF. 2001. Crystal structure of the ribosome at 5.5 Å resolution. *Science* **292:** 883–896.